Hyaluronan as Carrier of Carboranes for Tumor Targeting in Boron Neutron Capture Therapy

Chiara Di Meo,[†] Luigi Panza,[‡] Donatella Capitani,[§] Luisa Mannina,[§,||] Alessandra Banzato,[⊥] Maria Rondina,[⊥] Davide Renier,[#] Antonio Rosato,[⊥,▽] and Vittorio Crescenzi*[,†]

Department of Chemistry, University of Rome "La Sapienza", P. le Aldo Moro 5, 00185 Rome, Italy, Dipartimento di Scienze Chimiche, Alimentari, Farmaceutiche e Farmacologiche, University of Piemonte Orientale "A. Avogadro", via Bovio 6, 28100 Novara, Italy, Institute of Chemical Methodologies, Consiglio Nazionale delle Ricerche, Research Area of Rome, Via Salaria km 29,300, 00016 Monterotondo Stazione, Rome, Italy, Dipartimento di Scienze e Tecnologie Agro-Alimentari Ambientali e Microbiologiche, University of Molise, 86100 Campobasso, Italy, Department of Oncology and Surgical Sciences, University of Padova, I-36128 Padova, Italy, Fidia Farmaceutici SpA, Via Ponte della Fabbrica 3/a, I-35031 Abano Terme, Padova, Italy, and Istituto Oncologico Veneto, Via Gattamelata 64, I-35100 Padova, Italy

Received July 28, 2006; Revised Manuscript Received November 3, 2006

Boron neutron capture therapy (BNCT) represents a promising approach for tumor therapy. A critical requirement for BNCT is tumor targeting, a goal that is currently addressed with the development of low and high molecular weight agents capable of interacting with receptors expressed by cancer cells. Here, we describe a new bioconjugate (HApCB) composed by *n*-propyl carborane linked to hyaluronan (HA) via an ester linkage for a degree of substitution of approximately 30%, leading to a water-soluble derivative. The structure and main physicochemical characteristics of the new HA derivative were determined by means of Fourier transform infrared, fluorescence, and ^{1}H, ^{13}C, and ^{10}B NMR analysis and are herein reported in detail. As HA is recognized by the CD44 antigen, densely populating the surface of many tumor cells, HApCB is expected to deliver boron atoms from the locally released carborane cages directly to target cells for antitumor application in BNCT. In vitro biological experiments showed that HApCB was not toxic for a variety of human tumor cells of different histotypes, specifically interacted with CD44 as the native unconjugated HA, and underwent uptake by tumor cells, leading to accumulation of amounts of boron atoms largely exceeding those required for a successful BNCT approach. Thus, HApCB may be regarded as a promising new BNCT agent for specific targeting of cancer cells overexpressing the CD44 receptor.

Introduction

Boron neutron capture therapy (BNCT)[1−4] constitutes a potentially interesting cancer therapeutic modality, based on the capacity of ^{10}B to capture thermal neutrons and to disintegrate, releasing high linear energy transfer (LET) α particles (^{4}He) and recoiling lithium-7 nuclei. The critical requirements for a successful BNCT treatment are mainly: (a) the boron-containing compound/material has to be delivered to the neoplastic tissue to realize a specific and selective tumor targeting, and (b) the amount of ^{10}B atoms concentrated inside/around the cancer cells must be sufficient for the therapeutic purpose. If these rather stringent conditions are met, then irradiation of a given tissue or organ with therapeutic doses of thermal/epithermal neutrons can lead to a selective, complete ablation of malignant cells.

Although clinical exploitation of the BNCT strategy is currently being carried out with low molecular weight boron delivery agents, such as sodium borocaptate and boronophenylalanine, new high molecular weight carriers (monoclonal antibodies, polymers, and growth factors) are under development, with the main goal to increase the tumor to healthy tissue accumulation ratio.[4]

To comply with requirements of having a delivery agent endowed with both tumor tissue selectivity and high boron carrier capacity, we reasoned that a potential choice would consist of linking carborane cages[4−6] via appropriate short spacers to hyaluronan (HA) chains, yielding a polymeric water-soluble drug carrier relevant to BNCT. In this regard, carborane cages contain a relatively high number of boron atoms per unit volume, while HA represents a promising vehicle for tumor-specific targeting.

HA, a linear polysaccharide formed by alternating D-glucuronic acid (GlcUA) and *N*-acetyl-D-glucosamine (GlcNAc) units, is a biocompatible polymer playing important roles in cell adhesion, growth, and migration and acting as a signaling molecule in cell motility, inflammation, wound healing, and cancer metastasis through its receptors, mainly the CD44 antigen.[7−9] Since CD44 is widely overexpressed in many cancer histotypes,[10] HA−drug bioconjugates should be markedly selective for tumor cells and provide advantages in drug solubilization, stabilization, localization, and controlled release. Notably, bioconjugates formed by different antineoplastic drugs

* Author to whom correspondence should be addressed. E-mail: vittorio.crescenzi@uniroma1.it.
[†] University of Rome "La Sapienza".
[‡] University of Piemonte Orientale "A. Avogadro".
[§] Institute of Chemical Methodologies, Consiglio Nazionale delle Ricerche.
[||] University of Molise.
[⊥] University of Padova.
[#] Fidia Farmaceutici SpA.
[▽] Istituto Oncologico Veneto.

10.1021/bm0607426 CCC: $37.00
Published on Web 01/19/2007

Scheme 1[a]

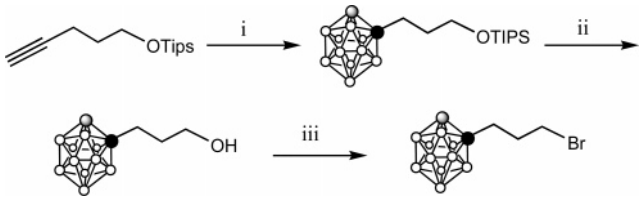

[a] (i) $B_{10}H_{14}$, CH_3CN/toluene, reflux, 56%; (ii) BuN_4F, THF/CH_3COOH, room temperature, 95%; (iii) PPh_3, CBr_4, CH_2Cl_2, 0 °C, 94%.

(butyric acid, paclitaxel, and doxorubicin) coupled to HA have already been proposed, demonstrating promising antitumor effects.[11−13]

Assuming that in BNCT the necessary amount of ^{10}B per gram of tumor is around 20−30 μg and assuming that a water-soluble HA−propylcarborane derivative (HApCB) with a degree of carborane substitution (DCS, i.e., moles of carborane linked per mole of HA repeating unit) of 30% can be prepared, a simple calculation shows that the amount of HApCB to be administered per gram of tumor is around 2 mg (considering that ^{10}B natural abundance is 20% and disregarding the weight of the spacer arms). Admittedly, this is not a small amount and implies that tumor targeting has been quantitative. However, higher DCS values can hardly lead to soluble HA derivatives due to the high hydrophobicity of the carborane moieties.

In this work we report the synthesis and the structural details, as assessed via NMR and IR spectroscopy, of a water-soluble HApCB having DCS close to 30%. The hypercoiling of such HA derivatives in aqueous solution was characterized qualitatively by monitoring pyrene fluorescence. Experiments conducted on tumor cells in vitro showed that HApCB was nontoxic, interacted with CD44 leading to receptor modulation, and heavily accumulated into cells, thus suggesting that the bioconjugate could represent a suitable tool for antitumor BNCT approaches.

Materials and Methods

Materials. Hyaluronic acid tetrabutylammonium salt (HATBA), M_η = 200 kDa, was provided by Fidia Advanced Biopolymers SRL, Abano Terme, Padua, Italy. Paclitaxel (Taxol) was from Bristol-Myers-Squibb Italia (Rome, Italy).

1-(3-Bromopropyl)-*o*-carborane (BrpCB) was prepared starting from triisopropyl-pent-4-ynyloxy-silane, which was allowed to react with the decaborane−acetonitrile complex. Deprotection of the resulting 1-(3-triisopropylsilanyloxy-propyl)-*o*-carborane with tetrabutylammonium fluoride in tetrahydrofuran/CH_3COOH gave the corresponding alcohol. Treatment with PPh_3/CBr_4 in dichloromethane according to a literature procedure[14] afforded 1-(3-bromopropyl)-*o*-carborane, as shown in Scheme 1. All other chemicals were reagent grade and were used without further purification.

Synthesis of the HApCB Derivative. The reagents HATBA and BrpCB, in *N*-methyl-pyrrolidinone (NMP) or similar solvents, quickly form physical gels at room temperature for HATBA concentrations higher than 2.5% w/v, preventing the reaction. Hence, we performed the HApCB synthesis using more dilute solutions, 1.7% w/v, at 37 °C; HATBA (∼50 mg) was dissolved in 3 mL of NMP until complete solubilization. Approximately 6.5 mg of BrpCB, previously dissolved in 200 μL of NMP, was then added. The reaction was performed under stirring for 40 h, the solution was then diluted by adding 4 mL of NMP, and 0.8 mL of NaBr saturated solution was added to have all hyaluronan-free carboxylate groups in the sodium salt form. The product was precipitated in acetone as a white solid and finally filtered with a 0.45 μm PTFE filter, washed three times with acetone/water 95:5 v/v to remove unreacted BrpCB and excess NaBr, and then washed with acetone twice. The product was dried at room temperature for 12 h, then stored at 4 °C. The reaction leading to the new HA derivative is shown in Scheme 2.

Methods. *Infrared Spectroscopy*. IR spectra were recorded with a Shimadzu 8300 Fourier transform infrared (FTIR) spectrometer in transmission mode (4 mg of the sample in 200 mg of dried KBr), collecting 32 scans in the 500−4000 cm^{-1} range, the resolution being 4 cm^{-1}. Spectra were normalized on the glycosidic stretching peak at 1151 cm^{-1}.

Fluorescence Spectroscopy. Fluorescence spectra of pyrene in the presence of increasing amounts of the HApCB derivative in aqueous solution were recorded using a Cary Eclipse (Varian) spectrophotometer working at an excitation wavelength of 334 nm. The pyrene probe (for fluorescence, ≥99.0%, Fluka) was stored under argon atmosphere to avoid oxidation. The stock solution of pyrene (5×10^{-7} M) was obtained by dissolving 2.50 mg of pyrene in 25 mL of acetone, then taking 25 μL and evaporating the solvent under nitrogen flux for 3 h. Finally, 25 mL of bidistilled water was added. Both solvents, acetone and water, were previously filtered (0.45 μm).

The HApCB stock solutions, 0.2, 2, and 20 mg/mL, were prepared in bidistilled water. Increasing amounts of these solutions were added to pyrene solution, and the excitation spectra were recorded at room temperature; the ratios between the intensity of the pyrene signals at 338 and 334 nm were calculated for all spectra.

The same experiment was carried out with unmodified hyaluronic acid sodium salt (HANa) as a control.

NMR Spectroscopy. Samples of HANa and HApCB, ∼4 mg, were solubilized in 700 μL of D_2O. A sample of BrpCB, 4 mg, was solubilized in 700 μL of dimethylsulfoxide (DMSO).

^1H and ^{13}C NMR experiments were performed at 27 °C on a Bruker AVANCE AQS 600 spectrometer operating at 600.13 and 150.95 MHz, respectively, and equipped with a Bruker multinuclear, *z*-gradient probe head. In all of the ^1H spectra, a soft presaturation of the HOD residual signal was applied.[15] ^{13}C NMR spectra were recorded using the following parameters: acquired points, 32 000; processed points, 64 000; recycle delay, 10 s; pulse width, 7 μs. The globally optimized alternating-phase rectangular pulses (GARP) sequence[16] for proton decoupling was applied during the acquisition.

^1H and ^{13}C assignments were obtained using $^1H-^1H$ correlation spectroscopy (COSY), $^1H-^1H$ total correlation spectroscopy (TOCSY), and $^1H-^{13}C$ heteronuclear single quantum coherence (HSQC) experiments with a *z*-gradient coherence selection. All two-dimensional (2D) experiments were carried out using 1024 data points in the f2 dimension and 512 data points in the f1 dimension; the recycle delay was 1s. The TOCSY experiment was performed with a spin−lock duration of 80 ms. The HSQC experiment was performed using a coupling constant of 150 Hz. The TOCSY and the HSQC experiments were processed in the phase-sensitive mode (time proportional phase increment (TPPI)) with 512 × 512 data points.

^1H and ^{13}C chemical shifts were reported in ppm with respect to 2,2-dimethyl-2-silapentane-5-sulfonate (DSS) sodium salt, used as an internal standard.

^{10}B NMR spectra were recorded at 64.48 MHz; chemical shifts were reported in ppm with respect to a 1 M boric acid/D_2O solution.

Pulsed-gradient spin echo (PGSE) experiments were performed with a pulsed field gradient unit producing a magnetic field gradient in the *z*-direction with a strength of 55.4 G cm^{-1}. The stimulated echo pulse sequence using bipolar gradients with a longitudinal eddy current delay was used. The strength of the sine-shaped gradient pulse, with a duration of 2 ms, was logarithmically increased in 16 steps, from 2% up to 95% of the maximum gradient strength, with a diffusion time of 600 ms and a longitudinal eddy current delay of 5 ms. After Fourier transformation and baseline correction, the diffusion dimension was processed using the diffusion-orderes spectroscopy (DOSY) subroutine of the Bruker Xwinnmr software package.

Tumor Cell Lines. HT-29, a colorectal adenocarcinoma, MCF-7, a mammary adenocarcinoma, and A2780 and OVCAR-3, ovary adeno-

Scheme 2. Schematic Representation of the Reaction between BrpCB and HATBA

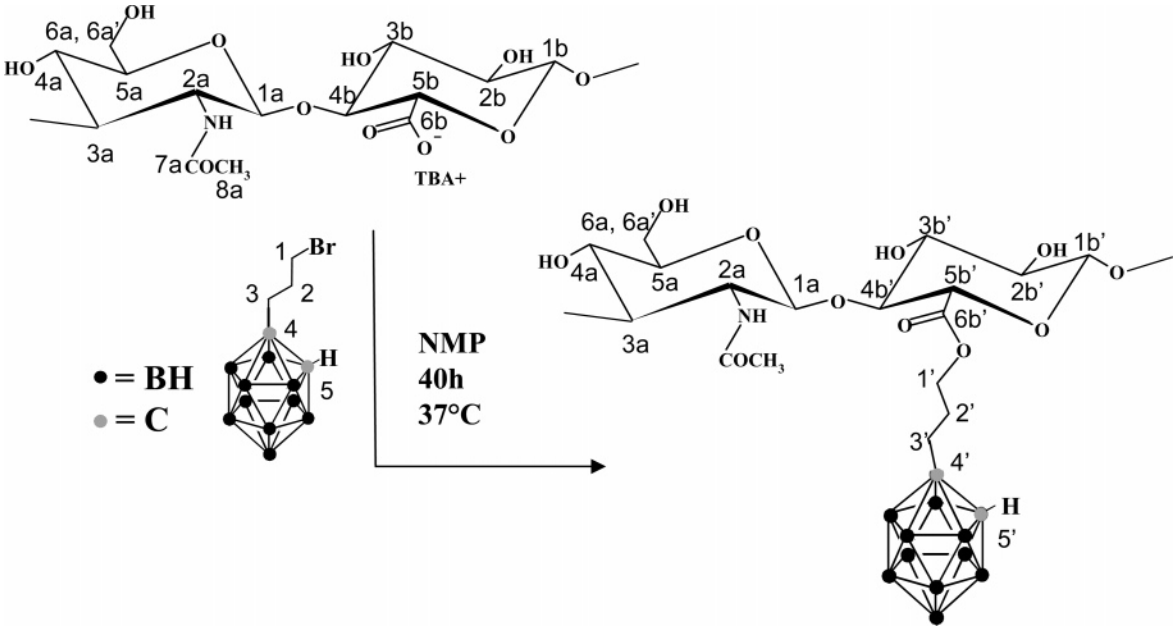

carcinomas, human tumor cell lines, were obtained from the American Type Culture Collection (ATCC). RT-112/84, a human bladder carcinoma epithelial tumor cell line, was obtained from the European Collection of Cell Cultures (ECACC). All cells were cultured in Eagle's minimal essential medium (EMEM, Sigma, St. Louis, MO) supplemented with 2 mM L-glutamine (Gibco BRL, Paisley, U. K.), 10 mM HEPES (PAA Laboratories, Linz, Austria), 150 U/mL streptomycin (Bristol-Mayers-Squibb Italia, Rome, Italy), 200 U/mL penicillin (Pharmacia and Upjohn, Milan, Italy), and 10% (v/v) heat-inactivated fetal calf serum (Gibco BRL), hereafter referred to as complete medium. After defrosting, each cell line was cultured for not more than 10 passages before being substituted with a fresh culture.

MTT (3-[4,5-Dimethylthiazol-2-yl]-2,5-diphenyl-tetrazolium bromide) Cytotoxicity Assay. The in vitro cytotoxicity of HApCB was studied in tumor cells using a slightly modified MTT assay.[13] Cells were resuspended in complete medium, seeded into 96-well flat-bottomed microtiter plates (1×10^4/well) for 24 h, and cultured (37 °C, 5% CO_2) in the presence of various HApCB concentrations for 72 h (final volume, 200 μL). Approximately 40 μL of a MTT solution (2.5 mg/mL in PBS) was then added to each well. After 3 h of incubation, the supernatant containing the unreacted dye was replaced with DMSO (100 μL/well), plates were vigorously shaken, and the absorbance at 570 nm was measured by a Titertek Multiscan reader within 1 h. Within each experiment, determinations were performed in triplicate, and experiments were repeated three times. The percentage of cell survival was calculated from the absorbance values as follows: $(A_{\text{tested}} - A_{\text{blank}})/(A_{\text{untreated control}} - A_{\text{blank}}) \times 100$, with A_{blank} referring to the absorbance of wells that contained only medium and MTT. A widely used antitumor cytotoxic agent, paclitaxel, was employed as a positive control for the tests.

Cell Staining, CD44 Receptor Modulation Assessment, and Quantification by Flow Cytometry Analysis. Evaluation of CD44 upregulation upon interaction with HApCB or HA was carried out on HT-29 and RT-112/84 cancer cells, as previously described.[13] Briefly, cells (3×10^5/sample) were incubated in 1 mL of complete medium containing 500 μg/mL HApCB or HA at 37 °C. At different time points, cells were resuspended in 100 μL of fluorexcence activated cell sorting (FACS) buffer (0.9% NaCl solution containing 2% bovine serum albumin and 0.02% NaN_3, both from Sigma) and stained at 4 °C for 20 min with a fluorescein isothiocyanate (FITC)-labeled anti-human CD44 mouse monoclonal antibody (1 μg/10^6 cells, clone J.173, Becton Dickinson, CA). Before analysis, the cells were washed twice, resuspended in FACS buffer, and analyzed with a flow cytometer, FACS-CALIBUR (Becton Dickinson). Data analysis was carried out using the Cell Quest software (Becton Dickinson). CD44 expression was compared to that of unstimulated cells.

CD44 receptor quantification by flow cytometry analysis was carried out on HT-29, MCF-7, OVCAR-3, and RT112/84 tumor cells using the QIFIKIT kit (DAKO), according to the manufacture's instructions.

Analysis of HApCB Uptake by Tumor Cells and Boron Atom Quantification. HT-29 and RT112/84 cells (2×10^6 cells/sample in 1 mL of complete medium) were incubated with 1 mg of HApCB at 37 °C to evaluate boron cell uptake. At different time points thereafter, samples were transferred at 4 °C to block drug uptake and washed twice with cold PBS, and pellets were immediately frozen in liquid nitrogen to be subsequently stored at −80 °C before analysis. Untreated cells were used as negative controls.

Each cell sample was dissolved with 500 μL of 50 mM Tris buffer solution, pH = 7.0, 0.1 w/v of sodium dodecyl sulfate (SDS) and 0.5 w/v of Triton-100. These solutions were diluted to 10 mL with distilled water, and then 2 mL of each solution was diluted again to 10 mL with distilled water for inductively coupled plasma atomic emission spectrometry (ICP-AES) analysis. Boron standards were prepared in the same Tris buffer solution, and 100 μL of 200 ppm yttrium was added as an internal standard in each sample and boron standard.

Results and Discussion

FTIR Analysis. The FTIR spectrum of the HApCB derivative was recorded in transmission mode (KBr) between 500 and 4000 cm^{-1} and is shown along with the HANa FTIR- spectrum in Figure 1. The HApCB spectrum displayed bands typical of a hyaluronan sample,[17] as shown in Figure 1, and two new peaks at 2596 and at 1737 cm^{-1} that we attributed to the B−H stretching of the carborane cage[5] and the C═O stretching of the carborane-propyl ester formed on the HA carboxylate after the reaction, respectively.

Fluorescence Experiments. Polyelectrolyte chains carrying hydrophobic substituents exhibit peculiar phenomena in aqueous solution traceable to micellization. Depending on the hydrophilic−lipophilic balance, these micelles unwind upon dilution at a characteristic concentration yielding open, solvated chains. Our fluorescence data show that this is the case for the hyaluronan derivative under consideration.

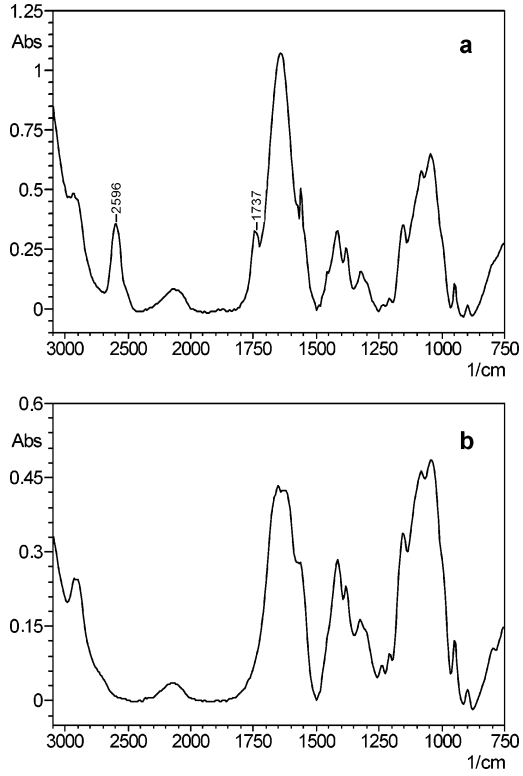

Figure 1. (a) FTIR spectrum of the HApCB derivative. The B−H stretching peak at 2596 cm^{-1} and the C═O stretching peak of the ester at 1737 cm^{-1} are clearly shown. (b) FTIR spectrum of HANa.

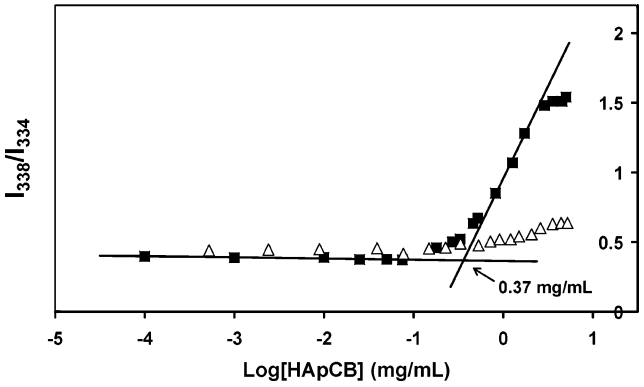

Figure 2. I_{338}/I_{334} variation of pyrene excitation spectra vs HApCB (■) and HANa (△) concentration in water. The intersection of the extrapolated straight line segments yields the onset CMC value (0.37 mg/mL) for the HApCB derivative.

As reported in the literature,[18] changes in the intensity of the pyrene probe fluorescence with polymer concentration in solution provide a method for the determination of the critical micelle concentration (CMC). In very dilute polymer solutions, below the CMC, the I_{338}/I_{334} ratio is characteristic of pyrene in aqueous media; with increasing polymer concentration above the CMC, the ratio increases, approaching the value of pyrene in a hydrophobic environment, typical of common micelles. Excitation spectra of the pyrene solution were recorded with increases in the HApCB concentration, from 10^{-5} up to 5 mg/mL; the I_{338}/I_{334} ratios were calculated and plotted versus polymer concentration, as shown in Figure 2. The intersection of the extrapolated straight line segments yields an estimated onset CMC value of 0.37 mg/mL for HApCB in water at room temperature. Because of the very low polymer concentration at the onset CMC, we are inclined to believe that HApCB forms intrachain micelles.

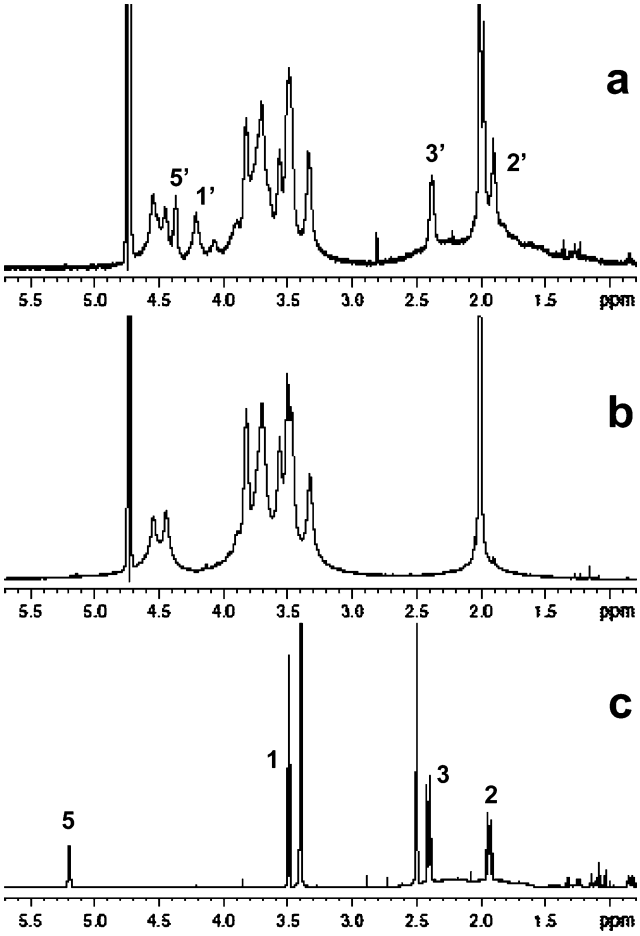

Figure 3. ^1H NMR spectra at 600.13 MHz and 27 °C of (a) the HApCB derivative in D_2O, (b) HANa in D_2O, and (c) BrpCB in DMSO-d_6 as a standard.

^1H and ^{13}C NMR Characterization of the HApCB Derivative. Figure 3a reports the ^1H NMR spectrum of the HApCB derivative; the ^1H spectra of (b) HANa and (c) a standard of BrpCB are also reported for comparison. In the spectrum of HApCB, besides the resonances of the HANa moiety, other resonances, respectively, labeled as 1′, 2′, 3′, and 5′, are observed. Moreover, a broad resonance, ranging from 1 to 2.6 ppm and produced by the protons attached to the boron atoms of the carborane cage, can also be observed,[19] as shown in Figure 3a.

The 2D-TOCSY map and the comparison with the chemical shifts of a standard of BrpCB allow the presence of the HApCB derivative to be revealed. The expanded TOCSY map reported in Figure 4a shows the correlation among the methylene 1′ at 4.213 ppm, the methylene 2′ at 1.900 ppm, and the methylene 3′ at 2.378 ppm; while this spin system matches the sketch reported in Scheme 2, the resonance of the methine 5′ at 4.370 ppm does not show any correlation. The ^1H assignments of the HApCB derivative and of the BrpCB used as a standard are reported in Table 1S in the Supporting Information. It is noteworthy that the chemical shift of the methylene 1′ in HApCB, which is close to the binding site, shows a marked downfield shift of approximately 0.719 ppm with respect to the corresponding one in free BrpCB, whereas the chemical shifts of methylenes 2′ and 3′, after the binding with HA, are poorly affected, showing upfield shifts of 0.036 and 0.028 ppm, respectively. Interestingly, protons belonging to the esterified glucuronic ring, labeled as 1b′, 2b′, 3b′, 4b′, and 5b′, can be distinguished from protons of the unsubstituted glucuronic ring

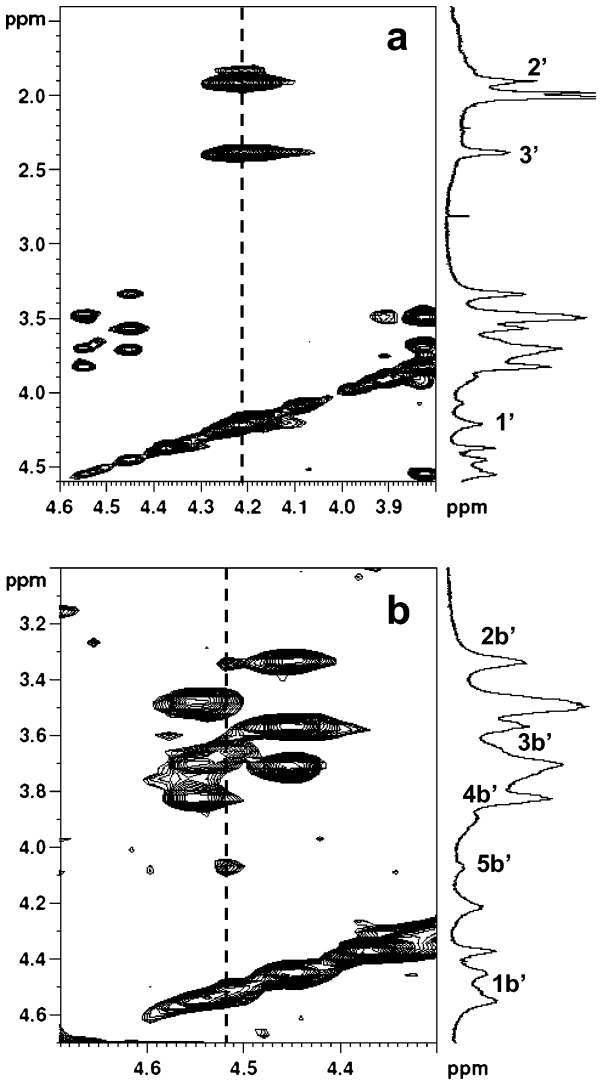

Figure 4. (a) 2D-TOCSY slice showing the correlation among methylene protons of the propyl moiety of the HApCB derivative. (b) 2D-TOCSY slice showing the correlation among protons of the glucuronic esterified ring of the HApCB derivative.

(1b, 2b, 3b, 4b, and 5b). The correlation among protons of the esterified glucuronic ring can be observed in the expanded TOCSY map reported in Figure 4b. Notably, proton 5b′, the closest to the binding site, is downfield shifted by 0.365 ppm with respect to the corresponding unsubstituted proton; proton 4b′ is also downfield shifted by approximately 0.11 ppm with respect to 4b; the chemical shifts of protons 3b′, 2b′, and 1b′ are poorly affected by the substitution. The HSQC map of HApCB is reported in Figure 5 along with the ^{1}H and ^{13}C spectra shown as projections; the ^{13}C assignment is also reported in Table 1S in the Supporting Information. In the same table, the ^{13}C assignment of the BrpCB standard, obtained with a HSQC map, is also reported. As expected, the methylene 1′ shows a marked downfield shift after the binding, from 34.08 to 67.20 ppm. This marked effect is due to the absence of the shielding effect of the bromine atom, the presence of the carboxyl 6b′ in the β position with respect to methylene 1, and, eventually, the effect of the oxygen in the α position. Methylene 2′ shows an upfield shift of 3.02 ppm after binding, possibly due to a γ-gauche effect[20] arising from the presence of the carboxyl 6b′ in the γ position; methylene 3′ is poorly affected by the binding.

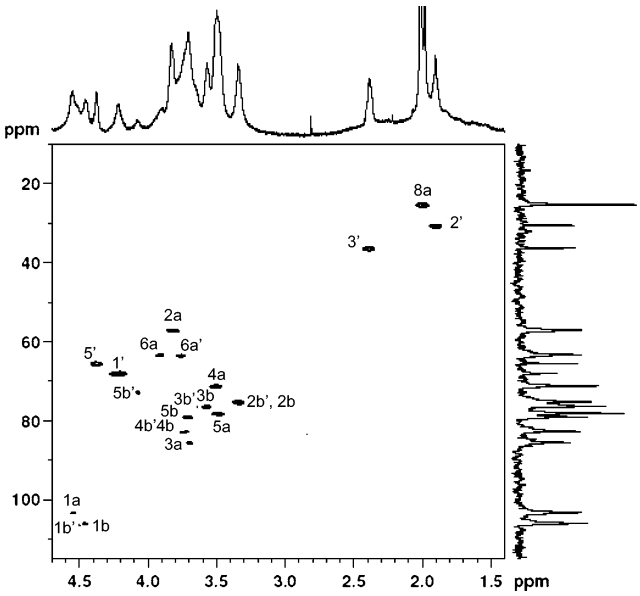

Figure 5. 2D ^{1}H−^{13}C HSQC map of the HApCB derivative in D_2O at 27 °C along with the full assignment. The ^{1}H and ^{13}C NMR spectra are reported as projections in the f2 and f1 dimensions, respectively.

After the binding, the ^{13}C chemical shift of carbon 5b′ shifts upfield from 78.22 to 75.16 ppm possibly due to a γ-gauche effects induced by the presence of carbon 1′. Carbon 4b′ shows a weak downfield shift from 81.89 to 82.20 ppm possibly due to a δ effect, whereas carbon 2b′ and 3b′ are almost unaffected by the binding.

In the ^{13}C spectrum of HApCB a resonance at 170.37 ppm due to carbon 6b′ after the formation of the ester linkage is observed (Supporting Information). This resonance is fully absent in the ^{13}C spectrum of the unsubstituted HA.

DOSY Measurements. It is well-known that molecular self-diffusion can be encoded into NMR data sets by means of a pulsed-gradient of the magnetic field.[21] Diffusion-ordered NMR spectroscopy[22] is a particularly convenient way of displaying the molecular self-diffusion information in a bidimensional array, with the ^{1}H NMR spectrum in one dimension and the self-diffusion coefficient in the other one. DOSY has been successfully used for the analysis of mixtures,[23] study of intermolecular interactions,[24,25] characterization of aggregates,[26] molecular weight determination of uncharged polysaccharides,[27] and optimization of the dialysis process of hyaluronic acid derivatives.[28,29]

In this regard, the linkage between propyl-carborane and HA can be further confirmed by means of a DOSY experiment. In fact, after the binding the diffusion coefficient of propyl-carborane bound to HA must be the same as that of HA, which is, obviously, much slower than the diffusion coefficient of BrpCB. Therefore, the presence of free BrpCB would be easily detectable in the DOSY map. In Figure 6 we report the DOSY map of the HApCB derivative, the ^{1}H spectrum being shown in the horizontal projection. The map demonstrates that resonances due to propyl-carborane display the same diffusion coefficient of the polysaccharide, therefore confirming the binding. Moreover, no low molecular weight impurities are found in the sample, as impurities would diffuse faster than the polysaccharide and would be easily observed in the DOSY map. Thus, the absence of impurities permits us to derive the true degree of substitution. In fact, after a careful baseline correction, the degree of substitution can be obtained by integrating the resonance at 3.33 ppm, due to the methines 2b and 2b′ of the polysaccharide, $I(2b + 2b')$, with respect to the

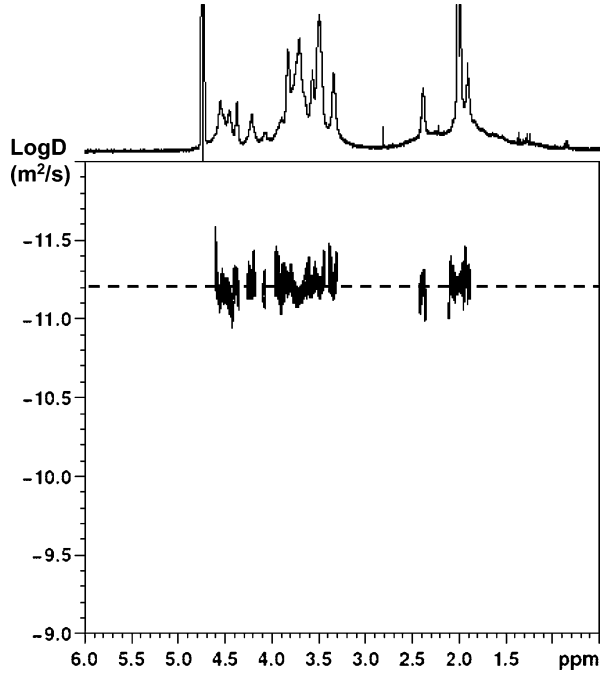

Figure 6. ^{1}H-detected DOSY map of the HApCB derivative in D_2O at 27 °C. The ^{1}H spectrum is shown as a horizontal projection.

resonance centered at 4.21 ppm, due to the methylene 1′ of the substituent, $I(1')$

$$\text{percentage of derivatization} = \frac{\frac{I(1')}{2}}{I(2b + 2b')} \times 100 = 28\%$$

Quantitative Analysis of Boron Content in HApCB by ^{10}B NMR. The spectrum of the HApCB derivative appears enlarged with respect to the spectrum of the standard compound, due to the binding with the polysaccharide, whereas, as expected, the chemical shift remains unchanged; see Figure 2S in the Supporting Information.

^{10}B NMR spectroscopy was also used to obtain a quantitative analysis of the boron content in HApCB. In fact the boron content in HApCB was evaluated from the ratio between the area of the resonance of $Na_2B_4O_7 \cdot 10H_2O$, used as a reference and calibrated to 1, and the area of the boron resonances of HApCB, which, according to the calibration, was 0.48. The calculation was performed according to the equation

$$\frac{\frac{5\text{ mg} \times 4}{\text{pM}(Na_2B_4O_7 \cdot 10H_2O)}}{\frac{4.4\text{ mg} \times 10x}{\text{pM(HApCB)}}} = \frac{1}{0.48}$$

where pM(HApCB) = 401 + 162x and x is the molar degree of derivatization.

The x value worked out to be 0.26. Note that this value is in good agreement with the molar degree of derivatization obtained by ^{1}H NMR, i.e., 0.28. Consequently, the amount of boron in 4.4 mg of HApCB was found to be 0.27 mg. Therefore the percentage in weight of boron in HApCB was 6% w/w.

Analysis of HApCB In Vitro Cytotoxicity. To test potential HApCB in vitro toxicity, CD44-expressing HT-29, MCF-7, OVCAR-3, and RT112/84 tumor cells and a CD44-negative A2780 ovarian cancer cell line were incubated with escalating concentrations of HApCB, native HA as a negative control, or a cytotoxic agent, paclitaxel, as a positive control. Table 1 reports results of the cell viability experiments following exposure to the highest concentration tested and shows that HApCB was extremely well tolerated, while paclitaxel strongly reduced cell survival. As expected, HA was nontoxic. These data suggest that HApCB is likely a biocompatible compound that could be safely used in vivo.

Table 1. Analysis of HApCB Cytotoxicity

	% of cell survival[a]		
cell line	HApCB	paclitaxel	HA
A2780 WT	100	5	100
HT-29	100	17	100
MCF-7	100	10	100
OVCAR-3	100	5	100
RT112/84	100	8	100

[a] Cell viability was assessed after exposure of cells to a 10 μg/mL concentration of each drug and evaluated by the MTT assay, as reported in the Materials and Methods section.

Assessment of CD44 Modulation by HApCB. CD44 HA receptor expressed on target cells may directly interact with the bioconjugate, resulting in an increased uptake of HApCB by tumor cells. Previous results showed that CD44 receptor was intensely expressed on part of RT-112/84 cells[13] and on all HT-29 cells (data not shown). To assess whether chemical coupling of carboranes to HA affected the binding of HApCB to CD44, RT112/84 and HT-29 cells were incubated with either the bioconjugate or HA, and CD44 expression and intensity were then analyzed at different time points. Exposure of the RT112/84 cell line to HA or HApCB brought about a similar initial down-modulation of the receptor, followed by an up-regulation in CD44 expression, thus indicating that the HA moiety of the bioconjugate is capable of freely interacting with the receptor (Figure 7a). Similarly, the intensity of CD44 expression on HT-29 cells underwent a progressive increase following exposure to both HA or HApCB (Figure 7b), thus demonstrating that the HA backbone not only stimulated more cells to express CD44 but also led to a higher number of receptors on single cells. Therefore, these results suggest that HApCB may undergo a selective uptake by HA receptor-expressing tumor cells, thus leading to the release of the carborane moieties in intracellular compartments upon hydrolytic breakdown of the molecule.

CD44 Receptor Quantification and Analysis of HApCB Upake. CD44 receptor modulation upon interaction with HApCB prompted us to determine the number of CD44 antigens presented by the different tumor cell lines tested, as it is conceivable that higher receptor expression would likely lead to the binding of more HApCB molecules and therefore to an increased uptake of boron atoms. To this end, HT-29, MCF-7, OVCAR-3, and RT112/84 tumor cells were cytofluorimetrically analyzed using a commercially available kit containing a set of beads mimicking cells labeled with a specific primary mouse monoclonal antibody as internal calibrators. Results of these experiments are reported in Table 2 and showed that HT-29, MCF-7, and OVCAR-3 tumor cells expressed a very high number of CD44 antigens, while RT112/84 bladder cancer cells, albeit positive, presented at least 10-fold fewer receptors on their outer membrane.

Next, we selected HT-29 and RT112/84 cell lines for subsequent HApCB uptake experiments. Cell samples were incubated with a saturating concentration of HApCB and then tested at different times for boron content using ICP-AES. HApCB uptake was very rapid during the first 15 min of incubation, reached a plateau after 60 min, and then declined very slowly up to 120 min, the last time point tested (data not

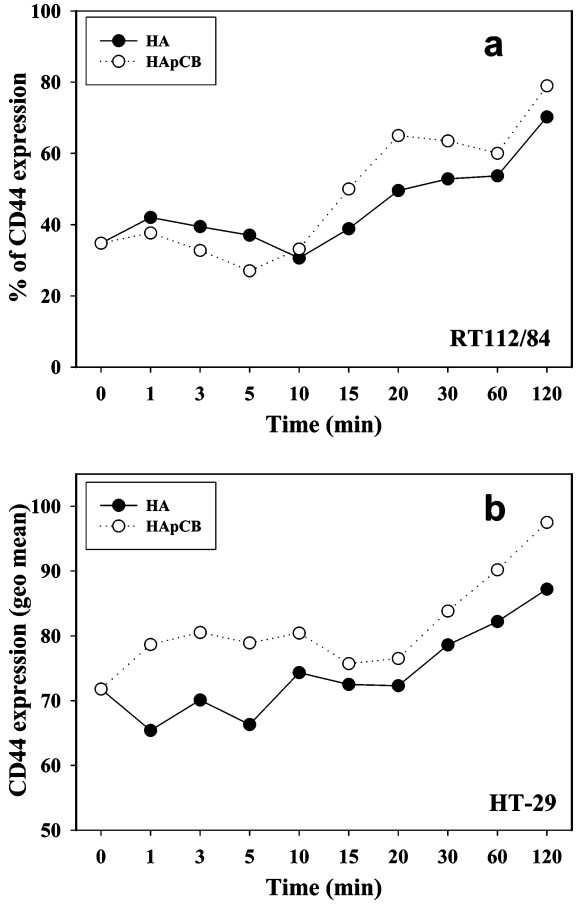

Figure 7. Flow cytometry analysis of CD44 modulation in (a) RT-112/84 and (b) HT-29 tumor cells. Evaluation of CD44 modulation upon interaction with HApCB or HA was carried out by incubating cancer cells with compounds at 37 °C. At different time points, cells were stained with a FITC-labeled anti-human CD44 mouse mAb, as reported in the Materials and Methods section. Data are expressed as (a) the percentage of cells expressing the CD44 receptor or (b) the fluorescence intensity.

Table 2. Quantitative Analysis of Cell Surface CD44 Receptors

cell line	number of CD44 (ABC)[a]
HT-29	158.292
MCF-7	124.081
OVCAR-3	286.762
RT112/84	13.775

[a] The CD44 receptor number was expressed in antibody-binding capacity (ABC) units calculated by flow cytometry analysis using the QIFIKIT kit, as described in the Materials and Methods section.

shown). At 1 h of incubation, the estimated boron contents for HT-29 and RT112/84 tumor cells were 8.2 and 11.7 mg/10^9 cells, respectively. These values deserve some consideration. We are aware that the concentration of HApCB employed in our experimental conditions was very high and that further analyses have to be conducted using lower compound amounts. Nonetheless, the enormous quantity of boron atoms incorporated by cells, which are hundreds of folds higher than those minimally required for BNCT, suggest that even much lower HApCB concentrations would be sufficient to deliver enough boron atoms to target cells. Second, CD44 receptor is expressed or overexpressed by a vast variety of tumor histotypes, thus implying that HApCB might find a broad application in cancer therapy. Finally, uptake results obtained with RT112/84 suggest that HApCB incorporation does not seem to depend on receptor density; in this regard, other mechanisms, such as very rapid CD44 recycling on the cell membrane, could compensate for low expression, ultimately leading to the accumulation of sufficient boron atoms for BNCT application, thus not limiting the approach with HApCB only to tumors overtly overexpressing the CD44 receptor.

Conclusions

In this paper we described the synthesis and preliminary biological characterization of HApCB, a new HA derivative carrying carborane cages, which appears particularly well-suited for antitumor BNCT approaches. Indeed, experiments outlined in this study allow us to draw a series of final conclusions. 3-Bromopropylcarborane, prepared as indicated in Scheme 1, easily reacted with the tetrabutylammonium salt of hyaluronan in *N*-methylpyrrolidone at 37 °C, yielding a partial ester of the glycosaminoglycan (Scheme 2). As assessed by 1D and 2D ^{1}H and ^{13}C NMR spectroscopy, an up to a 30% degree of substitution was still compatible with structure and water solubility, while higher carborane substitutions led to water-insoluble samples. Fluorescence data indicated that the HA partially esterified chains, for polymer concentrations higher than 0.4 mg/mL, assumed a globular conformation allowing pyrene molecules to be solubilized and to experience a hydrophobic environment provided by the carborane moieties. Biological studies disclosed that HApCB was biocompatible and well tolerated by several tumor cell lines, retained the capacity to specifically interact with CD44 receptor, and be internalized in high amounts, leading to an elevated boron atom content within cells. Therefore, HApCB may be considered as a new promising BNCT agent, endowed with both tumor targeting characteristics and a high ^{10}B atom carrier capacity, important features that should increase the therapeutic efficacy and have reduced side effects.

Acknowledgment. This work has been carried out with the financial support of Fidia Farmaceutici SpA, Abano Terme, Padua, Italy.

Supporting Information Available. ^{1}H and ^{13}C assignment of the HApCB derivative in D_2O and BrpCB in DMSO-d_6 at 27 °C, ^{13}C NMR spectrum of the HApCB derivative in D_2O at 27 °C, and ^{10}B spectra at 27 °C of the HApCB derivative in D_2O and BrpCB in DMSO-d_6. This material is available free of charge via the Internet at http://pubs.acs.org.

References and Notes

(1) Hawthorne, M. F.; Maderna A. *Chem. Rev.* **1999**, *99*, 3421−3434.
(2) Soloway, A. H.; Tjarks, W.; Barnum, B. A.; Rong, F.; Barth, R. F.; Codogni, I. M.; Wilson, J. G. *Chem. Rev.* **1998**, *98*, 1515−1562.
(3) Barth, R. F.; Coderre, J. A.; Vicente, M. G. H.; Blue, T. E. *Clin. Cancer Res.* **2005**, *11*, 3987−4002.
(4) Wu, G.; Barth, R. F.; Yang, W.; Lee, R. J.; Tjarks, W.; Backer, M. V.; Backer, J. M. *Anticancer Agents Med. Chem.* **2006**, *6*, 167−84.
(5) Valliant, J. F.; Guenther, K. J.; King, A. S.; Morel, P.; Schaffer, P.; Sogbein, O. O.; Stephenson, K. A. *Coord. Chem. Rev.* **2002**, *232*, 173−230.
(6) Different examples of carborane−carbohydrate conjugates have appeared in the literature in which the sugars were typically mono- or disaccharides. For examples, see: (a) Giovenzana, G. B.; Lay, L.; Monti, D.; Palmisano, G.; Panza, L. *Tetrahedron* **1999**, *55*, 14123. (b) Ronchi, S.; Prosperi, D.; Compostella, F.; Panza, L. *Synlett* **2004**, *6*, 1007−1010. (c) Tietze, M. L.; Griesbach, U.; Schuberth, I.; Bothe, U.; Marra, A.; Dondoni, A. *Chem.−Eur. J.* **2003**, *9*, 1296 and references therein. (d) Basak, P.; Lowary, T. *Can. J. Chem.* **2002**, *80*, 943. To our knowledge, only two examples in which a carborane has been conjugated with a polysaccharide (dextran) have been

reported: (e) Olsson P.; Gedda L.; Goike H.; Liu L.; Collins V.; Pontén J.; Carlsson J. *Anti-Cancer Drug Des.* **1998**, *13*, 279−289. (f) Tolmachev, V.; Bruskin, A.; Sjöberg, S.; Carlsson, J.; Lundqvist, H. *J. Radioanal. Nucl. Chem.* **2004**, *261*, 107−112.
(7) Aruffo, A.; Stamenkovic, I.; Melnick, M.; Underhill, C. B.; Seed, B. *Cell* **1990**, *61*,1303−1313.
(8) Toole, B. P. *Nat. Rev. Cancer* **2004**, *4*, 528−539.
(9) (a) Knudson, W.; Knudson, C. B. The Hyaluronan Receptor, CD44. http://www.glycoforum.gr.jp/science/hyaluronan/HA10/HA10E.html. (b) Knudson, W.; Knudson, C. B. The Hyaluronan Receptor CD44−An Update. http://www.glycoforum.gr.jp/science/hyaluronan/HA10a/HA10aE.html.
(10) Marhaba, R.; Zoller, M. J. *Mol. Histol.* **2004**, *35*, 211−231.
(11) Leonelli, F.; La Bella, A.; Francescangeli, A.; Joudioux, R.; Capodilupo, A. L.; Quagliariello, M.; Migneco, L. M.; Marini Bettolo, R.; Crescenzi, V.; De Luca, G.; Renier, D. *Helv. Chim. Acta* **2005**, *88*, 154−159.
(12) Jaracz, S.; Chen, J.; Kuznetsova, L. V.; Ojima, I. *Bioorg. Med. Chem.* **2005**, *13*, 5043−5054.
(13) Rosato, A.; Banzato, A.; De Luca, G.; Renier, D.; Bettella, F.; Pagano, C.; Esposito, G.; Zanovello, P.; Bassi, P. F. *Urol. Oncol.* **2006**, *24*, 207−215.
(14) Malmquist, J.; Sjoberg, S. *Inorg. Chem.* **1992**, *31*, 2534−2531.
(15) Guerènon, M.; Plateu, P; Decorps, M. *Prog. Nucl. Magn. Reson. Spectrosc.* **1991**, *23*, 135−109.
(16) Shaka, A. J.; Barker, P. B.; Freeman, R. J. *J. Magn. Reson.* **1985**, *64*, 547−552.
(17) Haxaire, K.; MaréChal, Y.; Milas, M.; Rinaudo, M. *Biopolymers* **2003**, *72*, 10−20.
(18) Astafieva, I.; Fu, Zhong, X.; Eisenberg, A. *Macromolecules* **1993**, *26*, 7339.
(19) Vyakaranam, K.; Rana, G.; Ratanasuwan, A.; Hosmane, S. N.; Maguire, J. A.; Hosmane, N. S. *Organometallics* **2002**, *21*, 3905−3912.
(20) Tonelli, A. E. The Synthesis and Reactions of Organic Compounds. In *NMR Spectroscopy and Polymer Microstructure*; VCH: New York, 1989; Chapter 8, p 385.
(21) Stejskal, E. O.; Tanner, J. E. *J. Chem. Phys.* **1965**, *42*, 288−292.
(22) Morris, K. F.; Johnson, C. S. *J. Am. Chem. Soc.* **1992**, *114*, 3139−3141.
(23) Morris, K. F.; Stilbs, P.; Johnson, C. S. *Anal. Chem.* **1994**, *66*, 211−215.
(24) Kapur, G. S.; Cabrata, E. J.; Berger, S. *Tetrahedron Lett.* **2000**, *41*, 7181−7185.
(25) Viel, S.; Mannina, L.; Segre, A. L. *Tetrahedron Lett.* **2002**, *43*, 2515−2519.
(26) Morris, K. F.; Johnson, C. S. *J. Am. Chem. Soc.* **1993**, *115*, 4291−4299.
(27) Viel, S.; Capitani, D.; Mannina, L.; Segre, A. L. *Biomacromolecules* **2003**, *4*, 1843−1847.
(28) Crescenzi. V.; Francescangeli, A.; Taglienti, A.; Capitani, D.; Mannina, L. *Biomacromolecules* **2003**, *4*, 1045−1054.
(29) Di Meo, C.; Capitani, D.; Mannina, L.; Brancaleoni, E.; Galesso, D.; De Luca, G.; Crescenzi, V. *Biomacromolecules* **2006**, *7*, 1253−1260.

BM0607426